INVESTIGATING THE ROLE OF ADAM10 AS A RECEPTOR FOR STREPTOCOCCAL PNEUMOLYSIN

By Rinke N. Nieuwschepen, performed at the group of Dr. A. N. Spaan, Department of Medical Microbiology, University Medical Center Utrecht, 16-08-2023

Contents

Abbreviations

- ADAM10 = A Disintegrin And Metalloprotease 10
- AT = α-toxin
- Cat # = catalog number
- CDC = cholesterol-dependent cytotoxin
- CPS = capsular polysaccharides
- DMEM = Dulbecco's modified eagle medium
- FCS = fetal calf serum
- GMF = geometric mean fluorescence
- ICE = Interference of CRISPR Edits
- NTC = non-targeting control
- PdB = PLY toxoid B
- PLY = pneumolysin
- PM = plasma membrane
- SABC = specific antibody-binding capacity
- sgRNA = synthetic guide RNA
- URT = upper respiratory tract

Layperson's Summary

The current study is focused on the bacterium Streptococcus pneumoniae. This bacterium is a leading cause of many serious diseases such as inflammation of the meninges and lungs. Streptococcus pneumoniae produces a toxin called pneumolysin (PLY). This toxin can form pores in the cell membrane that will kill the cell at high enough concentrations. PLY makes these holes by binding to cholesterol, which is an important component of the cell membrane. However, cholesterol is quite well hidden in the membrane. Directly binding cholesterol might be difficult for PLY. Many different toxins make use of so-called receptors to mediate their binding to a target cell. Receptors can be sugars or proteins that stick out from the cell membrane. We expect PLY to also use a receptor to help with its binding to cholesterol. A receptor is a great target for therapeutics. The binding of a toxin to a receptor can be stopped using drugs, which makes the toxin less effective. A candidate receptor for PLY is the protein A Disintegrin and Metalloprotease 10 (ADAM10). This protein is present on the outside of the cell membrane. We wanted to study if ADAM10 is used by PLY as a receptor. We expected that it is easier for PLY to bind to cells that express a high amount of ADAM10. This would make the cells more sensitive to PLY. To test this, we measured the amount of ADAM10 on the surface of various types of cells, as well as their sensitivity to PLY. We found that there is no correlation between the amount of ADAM10 present on the cell surface and cell sensitivity to PLY. A major downside of this experiment, however, is the fact that these cells produce many different proteins besides ADAM10. Therefore, we had to make sure that our measurements were only influenced by a change in the amount of ADAM10. We wanted to study the same cell type but with different quantities of produced ADAM10. To do this, we first edited the DNA of the cells, making them incapable of producing ADAM10. We then compared the sensitivity of cells to PLY between the normal cells and the cells without ADAM10. This way we could study the specific effects of ADAM10 on the sensitivity of cells to PLY.
We found that a loss of ADAM10 production did not change the sensitivity of these cells to PLY.
If PLY uses ADAM10 to bind more easily with cholesterol, the loss of ADAM10 production in cells would severely decrease their sensitivity to PLY. Therefore, we conclude that ADAM10 does not function as the receptor for PLY.

Abstract

Introduction: Pneumolysin (PLY) is a cholesterol-dependent-cytotoxin. It mediates host cell death by binding to the plasma membrane and oligomerizing into cytolytic pores. PLY has been found to induce ADAM10-dependent E-cadherin cleavage, suggesting that the metalloprotease ADAM10 might be a receptor for PLY. Therefore, this study aims to investigate the role of ADAM-10 as a receptor for PLY.

Methods: The surface expression of ADAM10 on multiple different epithelial and myeloid cell lines was measured. Lysis experiments with PLY were performed on these cell lines to study the sensitivity of cells in relation to their ADAM10 expression. Furthermore, the sensitivity of ADAM10-expressing rabbit erythrocytes and ADAM10-non-expressing human erythrocytes to PLY was compared. Lastly, ADAM10KO monoclonal cell lines were generated. Their sensitivity to PLY was measured and compared to the non-targeting control.

Results: ADAM10 surface expression did not correlate with cell sensitivity to PLY. Furthermore, rabbit and human erythrocytes demonstrated similar sensitivity to PLY. ADAM10KO cells did not demonstrate a physiologically relevant change in sensitivity to PLY.

Conclusion: Our findings strongly indicate that ADAM10 is not utilized as a high-affinity proteinaceous receptor of PLY.

Introduction

Streptococcus pneumoniae, commonly referred to as pneumococcus, is a gram-positive, extracellular pathogen. This opportunistic bacterium mainly colonizes the human upper respiratory tract (UTR), with 27-65% of children and <10% of adults being carriers. This carriage is the result of a commensal relationship. Dissemination of this bacterium is a leading cause of a broad range of bacterial infections such as sepsis, otitis media, meningitis, and community-acquired pneumoniae.

The usage of antibiotics and pneumococcal conjugate vaccines has significantly reduced the burden of this bacteria. However, genomic remodeling by this bacterium enables the development of resistance to commonly used antibiotics. Furthermore, serotypes differentiate significantly in their capsular polysaccharides (CPS) expression, of which most are not included in the current vaccines. As a result of the high burden of disease and its adaptability, the bacterium was declared one of the 12 priority pathogens by the World Health Organization in 2017.

S. pneumoniae expresses a large variety of virulence factors aiding its colonization of the host. Such virulence factors include the CPS, a multitude of glycosaminidases, adherence proteins, and multiple different choline-binding proteins (CBP) (1). One such CBP is LyTA, which induces autolysis (2). LyTA-mediated autolysis releases pneumolysin (PLY), one of the most important virulence factors of *S. pneumoniae*. PLY, a 53kDa pore-forming toxin (PFT), is involved in nearly every stage of the infection and transmission of *S. pneumoniae* (3). The primary functions of PLY include cytotoxic and pro-apoptotic activities towards many different host cells, the depletion of complement proteins from serum, and inducing inflammation (1). PLY is a PFT belonging to the cholesterol-dependent-cytotoxin (CDC) family. Its ability to bind with cholesterol allows PLY to target virtually every cell type found in the human body, demonstrated by its broad function in the multiple steps of infection (4). While most PFTs exploit high-affinity receptors to mediate their binding to the target membrane, no such receptor has yet been identified for PLY (5).

After autolysis, the now soluble PLY monomers interact with the host cells' plasma membrane (PM) by binding the cholesterol residues. They then multimerize, forming consecutively early and late pre-pore complexes. The complexes subsequently insert themselves into the PM to form a large transmembrane pore. The diameter of the late pre-pore complex varies, with the complex consisting of 40-44 monomers. After insertion of the pre-pore complex into the membrane, the transmembrane pore has a diameter of approximately 25 nm. This allows for the efflux of potassium ions, the influx of calcium ions, and the exchange of small molecules. At lytic concentrations of PLY, this exchange of ions and molecules results in massive mitochondrial damage, excessive pro-inflammatory signaling, and subsequent tissue injury. However, the sub-lytic PLY concentration stimulates plasma membrane repair and cell survival pathways.

Interestingly, PLY monomers do not always form pre-pores. At low concentrations of PLY, the monomers may form arc or slit-shaped oligomers on the target membrane (6,7). These formations have the ability to form pores, possibly of different sizes, permeability, and functional roles. At the early stages of infection, when the PLY concentration is relatively low, the pore formation may rely on the efficiency of the conversion from these complexes into pre-pore structures. At a later stage of the infection, higher concentrations of PLY result in the binding of the monomers to the PM of the host cells. Here, the lysis will mostly depend on PLY's affinity for cholesterol (4). We speculate that a proteinaceous receptor could be involved in the conversion of these arc or slit-shaped oligomers to pre-pore complexes, acting as a catalyst of sorts.

PLY has been shown to bind with other host molecules besides cholesterol. PLY binds the mannose receptor C type 1 expressed on the cell surface of certain types of immune cells in the airways such as macrophages and dendritic cells. Furthermore, PLY is capable of binding with the Fc portion of IgG, eliciting C1q recruitment and subsequent serum complement depletion. Lastly, it was suggested that PLY can bind host cell glycans such as divalent-LewisX (4). This data demonstrates that PLY is capable of directly binding with molecules other than cholesterol. Therefore, it is likely that PLY is capable of binding with a receptor to mediate its interaction with cholesterol.

Cholesterol availability is essential for the binding of PLY monomers. Cholesterol is deeply embedded within the PM and is therefore difficult to access (8). This hinders the binding of PLY to cholesterol. Furthermore, the glycocalyx attached to the outside of the plasma membrane sterically hinders the interaction between extracellular molecules and the plasma membrane (9). We postulate that this dense layer of sugars and proteins would prove a formidable barrier to PLY. Due to the poor accessibility of membranous cholesterol, we anticipate that a cell surface receptor facilitates its binding by PLY.

Interestingly, Inoshima et al. found the A Disintegrin And Metalloprotease 10 (ADAM10) to be activated by PLY. The PLY-dependent ADAM10 activity induced E-cadherin cleavage (10). The ADAM proteins are a family of enzymes of which ADAM10 is one of the most important members. ADAM10 has been described as a “molecular scissor” which plays a central role in the inflammatory response during sepsis. The protease cleaves numerous membrane protein substrates, including Notch, proinflammatory cytokines, and cadherins (11). Toxin-dependent ADAM10 activity has further been observed after intoxication with the *Staphylococcus aureus* α-toxin (AT), another PFT. ADAM10 is a well-established receptor for AT (10). Hence, we hypothesize PLY to utilize ADAM10 as its high-affinity proteinaceous receptor, similar to AT.

Altogether, the conversion of unbound PLY oligomers to pre-pore complexes, the inaccessibility of membranous cholesterol, and the ability of PLY to bind to different host molecules suggest that a receptor promotes the binding of PLY with membranous cholesterol. Since PLY induces ADAM10 activity similar to AT, we speculate that ADAM10 facilitates the interaction between PLY and plasma membranous cholesterol. Therefore, this work aims to elucidate the role of ADAM10 as a high-affinity receptor for PLY. Currently, no proteinaceous receptor has been identified for PLY. Therefore, this work may provide new potential therapeutic targets for the treatment of infections caused by *S. pneumoniae.*

Results

ADAM10 Cell Surface Expression Does Not Correlate With Pneumolysin Cytotoxicity

We first aimed to analyze whether PLY cytotoxicity is dependent on ADAM10 surface expression. Provided that ADAM10 is utilized by PLY as a high-affinity proteinaceous receptor to mediate the binding of PLY to the target membrane, a positive correlation between PLY cytotoxicity and ADAM10 surface expression is to be expected. To study such a correlation, the surface expression of ADAM10 and PLY's cytotoxicity (here denoted as the EC50, which is inversely correlated with cytotoxicity) were measured on a panel of humane, physiologically relevant cell lines. The panel consists of the cell lines A549, HaCaT, HEK293T, THP-1, and U937.

A549 is a human non-small cell lung cancer cell line, consisting of alveolar basal epithelial cells (12). These cells partially represent the cells encountered by *S. pneumoniae* during infection of the lung. The HaCaT cell line consists of human immortalized keratinocytes, the primary cell type found in the epidermis (13). As *S. pneumoniae* is commonly found on the skin in the poorer rural areas of Africa, this cell line is deemed highly relevant (14). The HEK293T cell line consists of immortalized human embryonic kidney cells. It has an epithelial morphology and is therefore partially representative of the epithelial cells in the upper respiratory tract (15). Both U937 and THP-1 cells are monocytic cell lines (16,17). PLY has demonstrated a multitude of effects on monocytes, marking them as cell types of interest (4).

A549 and HaCaT cells abundantly express ADAM10 on their surface (188493,1 specific antibody binding sites (SABC) and 136112,9 SABC, respectively). In contrast, THP-1, HEK293T, and U937 cells scarcely express ADAM10 (Figure 1a, THP-1: 55421,24 SABC, HEK293T: 36570,43 SABC, U937: 26793,45 SABC). Contrary to our expectations, the THP-1 cells were the most sensitive to PLY (EC50: 0,1369 ug/ml), followed by HaCaT (EC50: 0,3288 ug/ml), U937 (EC50: 0,3625 ug/ml), HEK293T (EC50: 0,3860 ug/ml), and A549 cells (EC50: 1,056 ug/ml), respectively (Figure 1b). Through a linear regression analysis, it is shown that PLY cytotoxicity does not correlate with the surface expression of ADAM10 ($P = 0,1461$) (Figure 1d). This suggests that ADAM10 is not exploited by PLY as a receptor in a surface expression-dependent manner. However, the studied cell lines have distinct membrane compositions and gene expressions. For example, it is thought that the difference in plasma membrane repair capacity of cell types, post-pore formation, can differentiate cell sensitivity to PLY (18). Therefore, we cannot exclude the involvement of ADAM10 in PLY cytotoxicity solely based on this data.

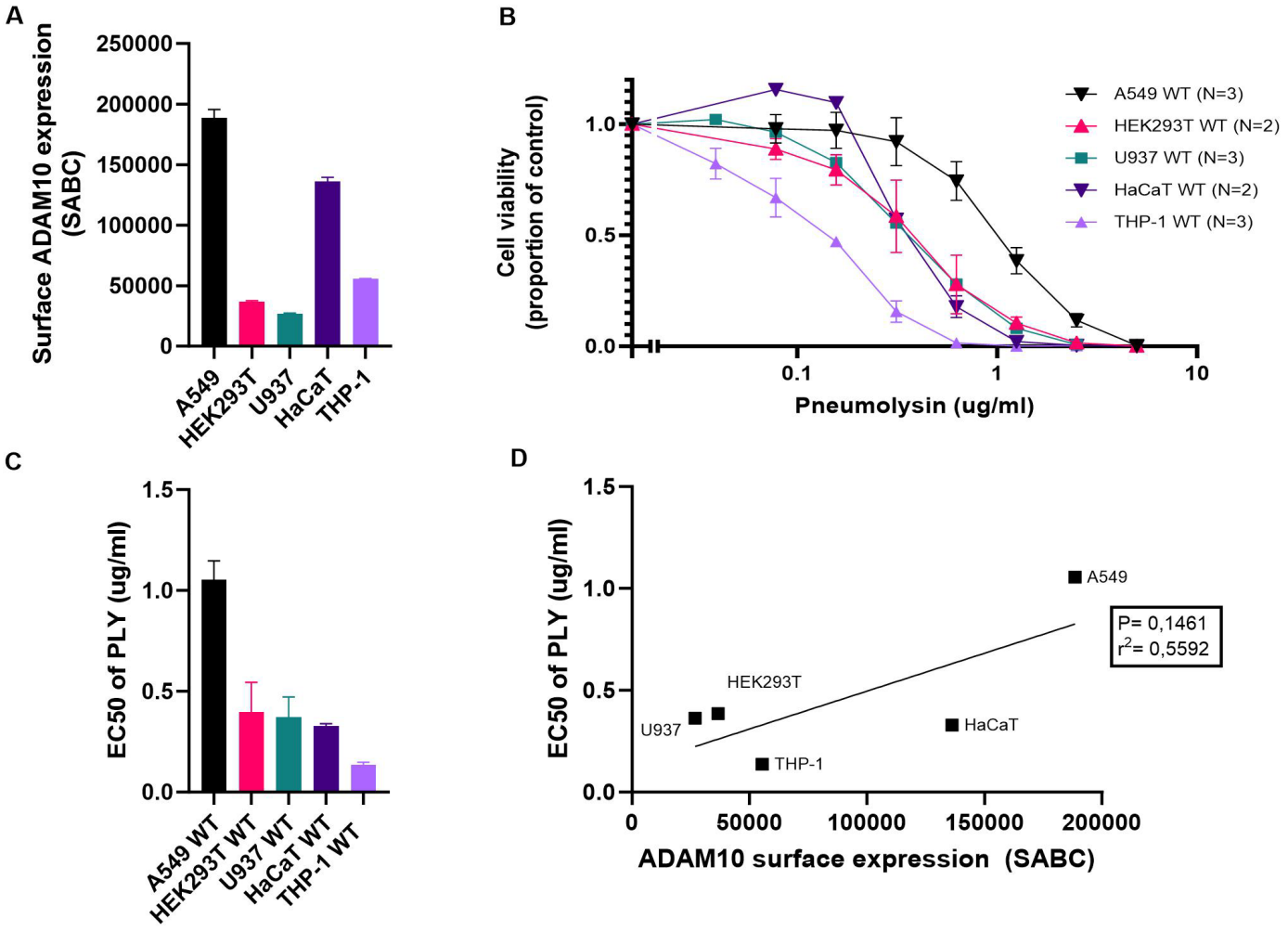

Figure 1 ADAM10 surface expression does not correlate with cell sensitivity to PLY. *(A) Cell surface expression of ADAM10, quantified as* Specific Antibody-Binding Capacity (SABC)*, on the HaCaT, A549, HEK293T, THP-1, and U937 cell lines. (B) Cell viability after 24 hours of intoxication with a serial dilution of PLY (A549, U937, THP-1 N=3; HEK293T, HaCaT N=2). (C) A549 is relatively less sensitive to PLY whereas THP-1 is relatively more sensitive, as depicted by their respective EC50 of PLY. (D) Linear regression analysis revealed no statistical correlation between the EC50 of PLY and ADAM10 cell surface expression (P = 0,1461).*

Rabbit And Human Erythrocytes Show Similar Sensitivity To Pneumolysin

As human erythrocytes do not express ADAM10, but rabbit erythrocytes do, a hemolysis assay comparing the sensitivity to PLY of these erythrocytes would mimic a knockout strategy. PLY was found to have similar cytotoxicity towards both human and rabbit erythrocytes (human erythrocytes EC50: 0,2752 ng/ml, rabbit erythrocytes EC50: 0,3645 ng/ml) (Figure 2). Similar cell sensitivity to PLY, regardless of ADAM10 surface expression, supports the notion that ADAM10 is not involved as a receptor for PLY.

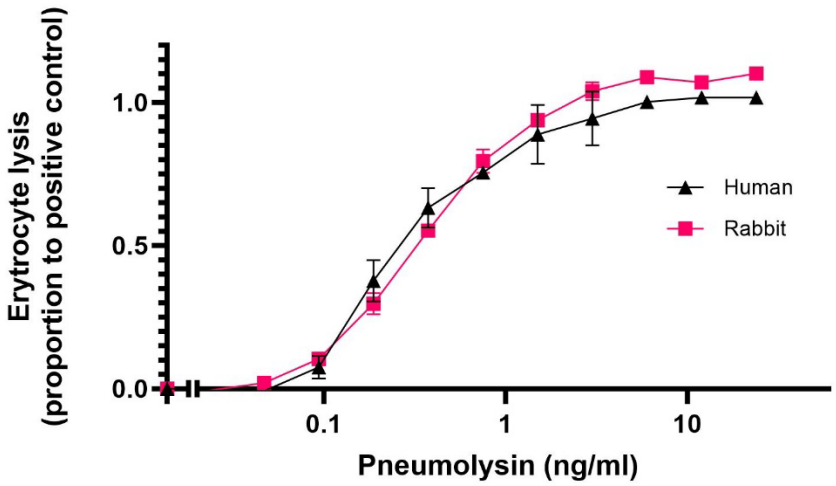

Figure 2 Human and rabbit erythrocytes have a similar sensitivity to PLY. *Lysis of human (black) and rabbit (pink) erythrocytes after 30 min of intoxication with a serial dilution of PLY.*

As the compared erythrocytes are isolated from different species, the expressed ADAM10 is not human. However, analysis reveals a 98,4% overlap between the amino acid sequence of human and rabbit ADAM10 (Figure S1). Furthermore, using the ADAM10-specific inhibitor GI254023X, it has been demonstrated that inhibition of ADAM10 on rabbit erythrocytes inhibits AT cytotoxicity, comparable to human ADAM10 (10). This indicates that rabbit ADAM10 studies are partially representative of the human condition.

Generation And Validation Of ADAM10 Knockout Cell Lines

To study the role of ADAM10 on sensitivity to PLY, A549 and THP-1 ADAM10 knockout cells were generated using CRISPR/Cas9 knockout technology (Figure S2). A non-targeting control (NTC), a synthetic guide RNA consisting of a random set of 20 nucleotides, was used to generate control cell lines. From the tested cell lines described above, the selection was made based on cell sensitivity to PLY and ADAM10 surface expression (Figure 1a). A549 cells express the highest quantity of cell surface ADAM10 and have previously been used to study PLY induced ADAM10 activity (10). Generating knockouts of ADAM10 in A549 cells will result in a large decrease in protein expression, which we hypothesize to translate into a large phenotypical change. THP-1 expresses less ADAM10 on its cell surface than A549 and HaCaT cells. However, the cell line has the highest sensitivity to PLY from the studied cell lines (Figure 1c). The relatively high sensitivity to PLY makes the THP-1 cell line an interesting model, as a significant shift in sensitivity might be observed when ADAM10 is knocked out. After the knockout procedure, cells were stained with either α-ADAM10 primary antibody, an isotype control, only the secondary antibody, or no antibodies. Flow cytometry analysis of the polyclonal populations revealed that the knockout efficiency of ADAM10 in the selected cell lines is exorbitant, whereas the NTC cell lines showed WT levels of ADAM10 (Figure 3ab, Figure S3).

100% of the A549 NTC cells were ADAM10 positive, and 98,4% of the A549 ADAM10KO of cells were deemed ADAM10 negative. For the THP-1 cells, the auto-fluorescent signal and the ADAM10 positive histograms partially overlap. 99,9% of NTC cells were deemed ADAM10 positive, and 1,89 % were deemed ADAM10 negative. For the THP-1 ADAM10KO cells, 99,5% were deemed ADAM10 negative, and 6,98 % were deemed ADAM10 positive. Regardless of the small overlap in populations, the ADAM10 knockout strategy was highly efficient in both cell lines. Therefore, monoclonal populations of these cells were generated using a limited dilution approach. Four monoclonal populations were

selected for each cell line, both the NTC and ADAM10KO variants, and further validated using both flow cytometry and genetic analyses.

The flow cytometry data of the monoclonal cell lines reflected the knockout efficiency measured in the polyclonal population. In all four monoclonal populations, for both A549 and THP-1, the ADAM10KO cell lines demonstrated a complete lack of ADAM10 cell surface expression. The NTC derived monoclonals, however, showed an ADAM10 surface expression comparable to the WT measurements (Figure 3c, Figure S4).

Interference of CRISPR Edits (ICE) analysis of genomic DNA was performed to further validate the ADAM10KO. This analysis aligns the DNA sequence of the knockout variant with that of the NTC. It then compares the sequencing traces to analyze whether editing has occurred, and on which positions. For each cell line, the four selected NTC's were compared with each ADAM10KO population. The insertion-deletion % for each successfully compared pair was 100%, meaning that these samples show insertions and/or deletions in every sequence measured. Deletions of more than 21 base pairs are counted towards a knockout score (Figure S5).

Cell lines were then selected for functional assays based on their (lack of) ADAM10 surface expression, ICE knockout score, and general growth speed. Based on these parameters, A549 NTC #2, A549 ADAM10KO #2, THP-1 NTC #4, and THP-1 ADAM10KO #1 were selected for further testing.

As previously mentioned, ADAM10 is a well-established receptor for AT. Therefore, intoxication of ADAM10KO cell lines with this toxin would confirm phenotypical changes. As expected, NTC cells exhibit a concentration–dependent decrease in cell viability after intoxication by AT. ADAM10KO cells do not exhibit this concentration-dependent decrease, indicating that the ADAM10 knockout has a functional impact on the cytotoxicity of AT (Figure 3d). It is highly anticipated that other pore-forming toxins that exploit ADAM10 as a receptor will display a similar phenotype on these cells.

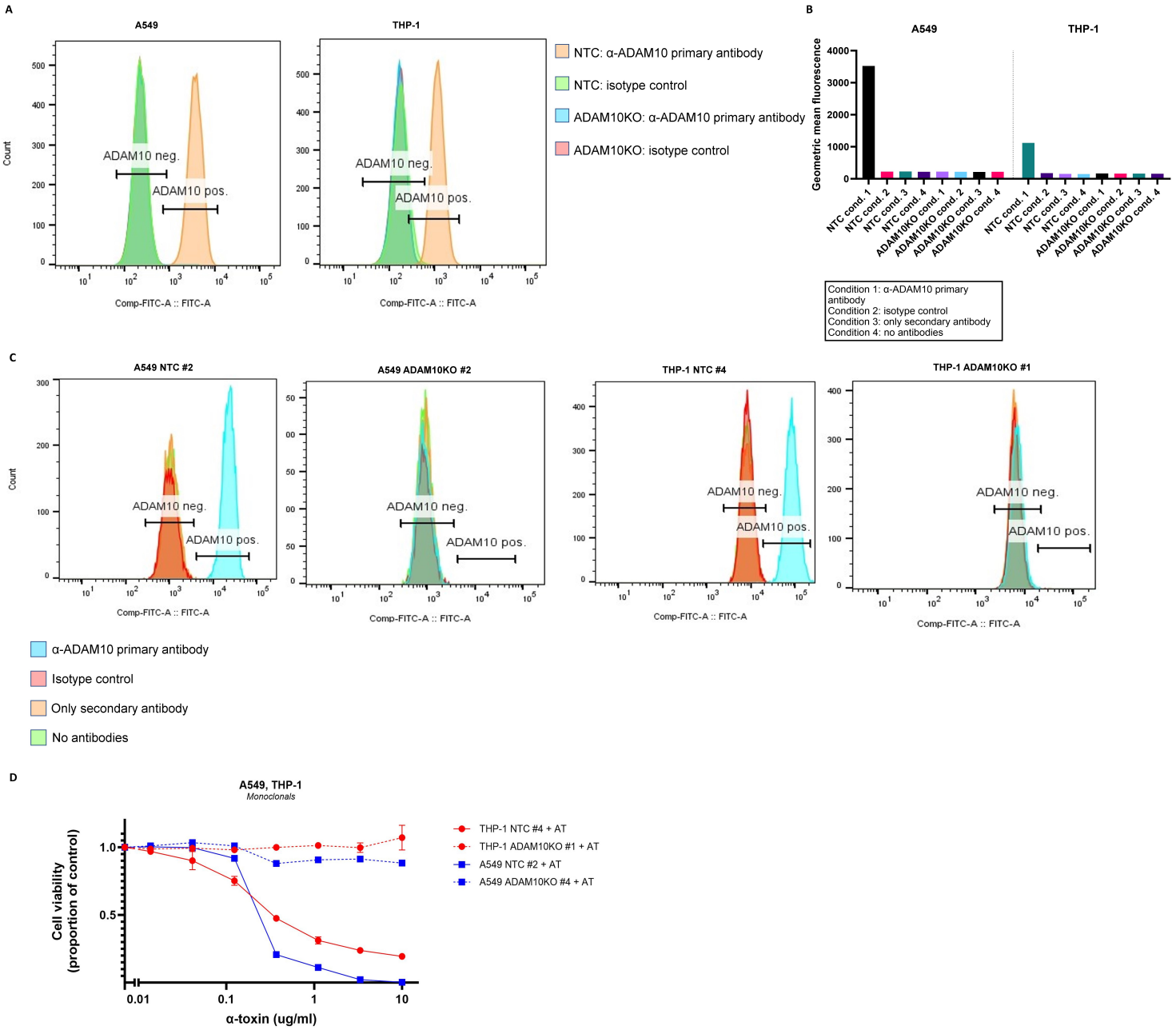

Figure 3 Monoclonal ADAM10KO populations show no ADAM10 surface expression and are functionally relevant. *(A) A549 and THP-1 NTC and ADAM10KO cells were stained with either an α-ADAM10 primary antibody or an isotype control. Flow cytometry revealed a high knockout efficiency and little aspecific binding, with the ADAM10KO histograms overlapping with the isotype control of the NTC cells. (B) Geometric mean fluorescence of the aforementioned flow cytometry measurements. Here data of additional controls are shown in the form of only secondary antibody and no antibody staining. (C) Flow cytometry data of monoclonal cell lines generated from NTC and ADAM10 knockout polyclonal cell lines. The same conditions described for the polyclonal analysis were applied here. The numbers of the monoclonals were assigned at random when selecting the four populations for further analysis. ADAM10KO cells were completely ADAM10 negative. (D) AT intoxication of NTC cells decreases the cell viability in a concentration depended manner. ADAM10KO monoclonals show resistance to AT intoxication.*

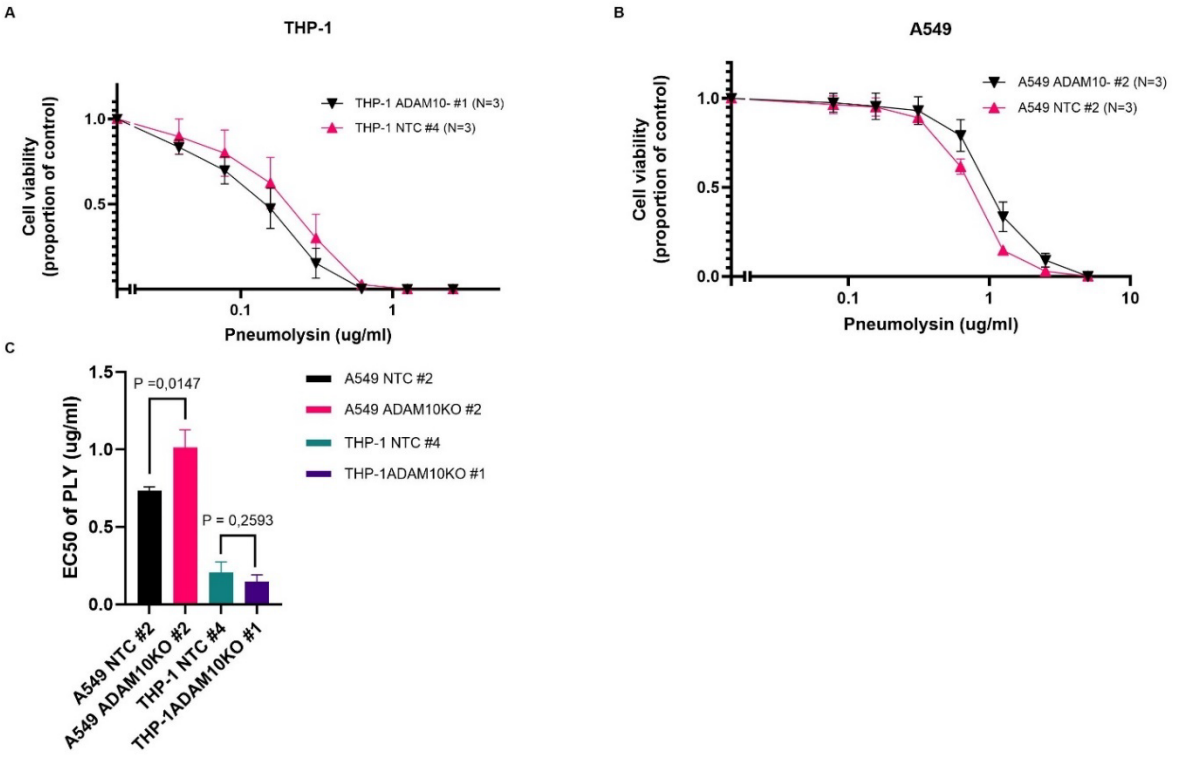

Figure 4 Cell sensitivity to PLY is not altered by ADAM10 knockout. *(A) The mean cell viability of THP-1 ADAM10KO (black) and NTC (pink) cells (N=3) (B) as well as the A549 cell lines (N=3) after intoxication with a serial dilution of PLY. (C) PLY cytotoxicity is decreased in A549 ADAM10KO cells but not in THP-1 ADAM10KO cells.*

ADAM10 Deficiency Does Not Cause Decreased Sensitivity To Pneumolysin

Next, PLY intoxication assays were performed on the generated ADAM10KO cells. The THP-1 ADAM10KO cells did not display a significant change in sensitivity to PLY (EC50 NTC: 0,1460 ug/ml; EC50 ADAM10KO: 0,2074 ug/ml; P = 0,259) (Figure 4a, c), comparable to the data generated by the rabbit (ADAM10 positive) and human (ADAM10 null) hemolysis assay (Figure 2). However, a small but significant difference in sensitivity to PLY was observed for the A549 cells, with the A549 ADAM10KO cells displaying a decrease in sensitivity to PLY (EC50 NTC: 0,7342 ug/ml; EC50 ADAM10KO: 1,012 ug/ml; P = 0,0147) (Figure 4b, c).

Discussion

In this study we aimed to characterize the role of ADAM10 as a high-affinity proteinaceous receptor for the *S. pneumoniae* PLY.

First, we measured the surface expression of ADAM10 on a panel of humane cell lines, and subsequently their sensitivity to PLY through the utilization of cytotoxicity assays. However, no correlation between the ADAM10 surface expression and PLY sensitivity could be distinguished. Furthermore, cellular sensitivity to PLY was measured in ADAM10 expressing and non-expressing cells. This was done by comparing either rabbit and human erythrocyte's sensitivity to PLY, or through the generation of ADAM10KO cells. Both comparisons showed no ADAM10-dependent cell sensitivity to PLY. Altogether, these results strongly indicate that ADAM10 does not function as a high-affinity receptor.

An interesting observation has been the small but significant change in sensitivity to PLY for the A549 cell line, where the ADAM10KO cells were shown to be less sensitive to PLY than the NTC. However, this change in sensitivity is deemed negligible when compared to the substantial change in AT sensitivity of the same cells. In case PLY utilizes ADAM10 as a receptor, similarly to AT, a comparable shift in cytotoxicity may be anticipated. Rather than ADAM10 functioning as a receptor for PLY on A549 but not on THP-1 cells, we hypothesize that observed change is a result of PLY induced ADAM10 activity. As previously described, PLY can induce ADAM10 activity resulting in the cleavage of a plethora of membrane proteins. This includes multiple adhesion molecules such as E-cadherin (19). We postulate that the ADAM10KO cells exhibit decreased cleavage of adherence proteins upon PLY stimulation. These cells would therefore be more adherent. As detached epithelial cells undergo anoikis, the reduction in sensitivity to PLY of ADAM10KO A549 cells may be partially attributed to their heightened adhesion (20). Furthermore, E-cadherin is involved in cell-cell contacts and stabilizes the actin cytoskeleton (21). Cleavage of E-cadherin destabilizes the actin cytoskeleton, inducing an apoptotic response (22). As ADAM10 activity aggravates the cytotoxicity of AT, it is likely that PLY induced ADAM10 activity would exhibit a similar phenotype (10). An ADAM10 specific inhibitor can be utilized to validate this hypothesis. By treating ADAM10 expressing cells with the inhibitor, the exhibited phenotype upon PLY exposure can be compared to ADAM10KO cells. As THP-1 cells are inherently non-adherent cells, this PLY induced ADAM10 cleavage of adherence proteins would not alter their cell viability.

Contrary to this hypothesis, under physiological conditions, E-cadherin inhibits cell proliferation, and ADAM10 promotes cell growth (23,24). Therefore, trying to explain these results solely based on PLY induced ADAM10 E-cadherin cleavage would be an oversimplification. Due to the broad range of ADAM10 substrates, it is challenging to isolate a single causal mechanism that elucidates the observed difference between the THP-1 and A549 cell lines.

Altogether, while there is a significant change in PLY cytotoxicity on A549 cells upon ADAM10 knockout, this change is not substantial enough to support the model of ADAM10 functioning as its receptor. Therefore, we can confidently conclude that ADAM10 does not function as a high-affinity receptor for PLY.

As of now, an explanation for the previously observed PLY-induced ADAM10 activity remains unclear, and no proteinaceous receptor has yet been identified for PLY (10). As previously stated, we deem it likely for PLY to utilize a receptor. The majority of PFTs exploit cell proteins or glycans as receptors (5). Furthermore, cholesterol is deeply embedded in the membrane and is difficult to access. A potential proteinaceous receptor for PLY could be the purinergic receptor P2X7. The contribution of purinergic

receptors to the cytolytic effects of PFTs has been a subject of ongoing discussion for some time (25). In its trimeric form, P2X7R is expressed on the cell surface as a transmembrane complex and binds extracellular ATP. Upon activation, the P2X7R oligomer undergoes conformational changes, allowing the exchange of ions by functioning as a channel. Upon P2X7R stimulation, downstream signaling can induce the activation of both the NLRP3 inflammasome and ADAM10. Furthermore, P2X7R stimulation has been demonstrated to decrease expression of E-cadherin (26–28). Previous studies have indicated that P2X7R co-localizes with PLY on neutrophils. Additionally, overexpression of P2X7 in the P2X7 null A549 cells enhanced PLY induced cell lysis (29). Based on literature we propose the following model (Figure 5). P2X7R could function as a high affinity proteinaceous receptor for PLY, acting as a catalysator for the binding to cholesterol and the formation of PLY pores (Figure 5a). These pores would then allow for the diffusion of ATP across the PM, activating P2X7R. Together, P2X7R would increase the cell sensitivity to PLY by mediating PLY pore formation and inducing pyroptosis upon activation. Alternatively, PLY could form pores in the membrane independent of P2X7R, induce an increase in extracellular ATP, and thereby induce P2X7R activity (Figure 5b). It is thought that AT dependent ADAM10 activity is a result of undefined lesions in the PM of the host cell, possibly mediated by a purinergic receptor (25). This supports the notion that PLY might function in a similar manner. Regardless of the mechanism, in this model activation of P2X7R is induced, leading to ADAM10 activity and pyroptosis.

P2X7 does not protrude far from the membrane. Its extracellular domain consists of 282 amino acids. In contrast, the extracellular domain of ADAM10 consists of 652 amino acids. Therefore, it might not function as a receptor (26,30). Additionally, Ca^{2+} influx alone is sufficient to induce ADAM10 activity (Figure 5c)(11). The formation of PLY pores, but also AT pores, might therefore induce ADAM10 activity by allowing this influx of Ca^{2+}. It has been suggested that AT dependent ADAM10 activity is either a result of the AT pore serving as an ion conduit or a dependency of AT on the presence of Ca^{2+} in order to induce ADAM10 activity (10). This hypothesis might also apply to PLY.

In order to verify this model, we aimed to generate P2X7KO cell lines. While successful editing of the P2RX7 gene was achieved, it was not possible to validate the P2X7 knockout at the protein level (Figure S6, S7). Optimization of both the P2X7 knockout and the validation protocols will facilitate our study of the role of P2X7 as a receptor for PLY. In case that P2X7 is found not to be a receptor for PLY, a broader approach in the form of a CRISPR screen could be applied to identify potential proteinaceous receptors. An alternative approach could be taking advantage of the non-pore forming mutant of PLY, PLY toxoid B (PdB). This mutant contains the $W_{433}F$ mutation, preventing the insertion of the toxin into the membrane. PdB can be utilized to analyze the binding of PLY to cell surface proteins (31). Incubating cells with GST tagged PdB, followed by a pull-down assay in combination with mass spectrometry, allows for the identification of protein binding targets that might function as a receptor (32).

In conclusion, our data strongly indicates that ADAM10 is not exploited by PLY as a high-affinity proteinaceous receptor. PLY-induced ADAM10 activity might aggravate PLY cytotoxicity without ADAM10 functioning as a receptor. A candidate of interest in PLY cytotoxicity is the purinergic receptor P2X7. There are multiple models to be explored for this protein which could affect PLY cytotoxicity. Future research should elucidate the role of P2X7 in PLY cytotoxicity or utilize either CRISPR screens or PdB assays to determine potential proteinaceous receptors.

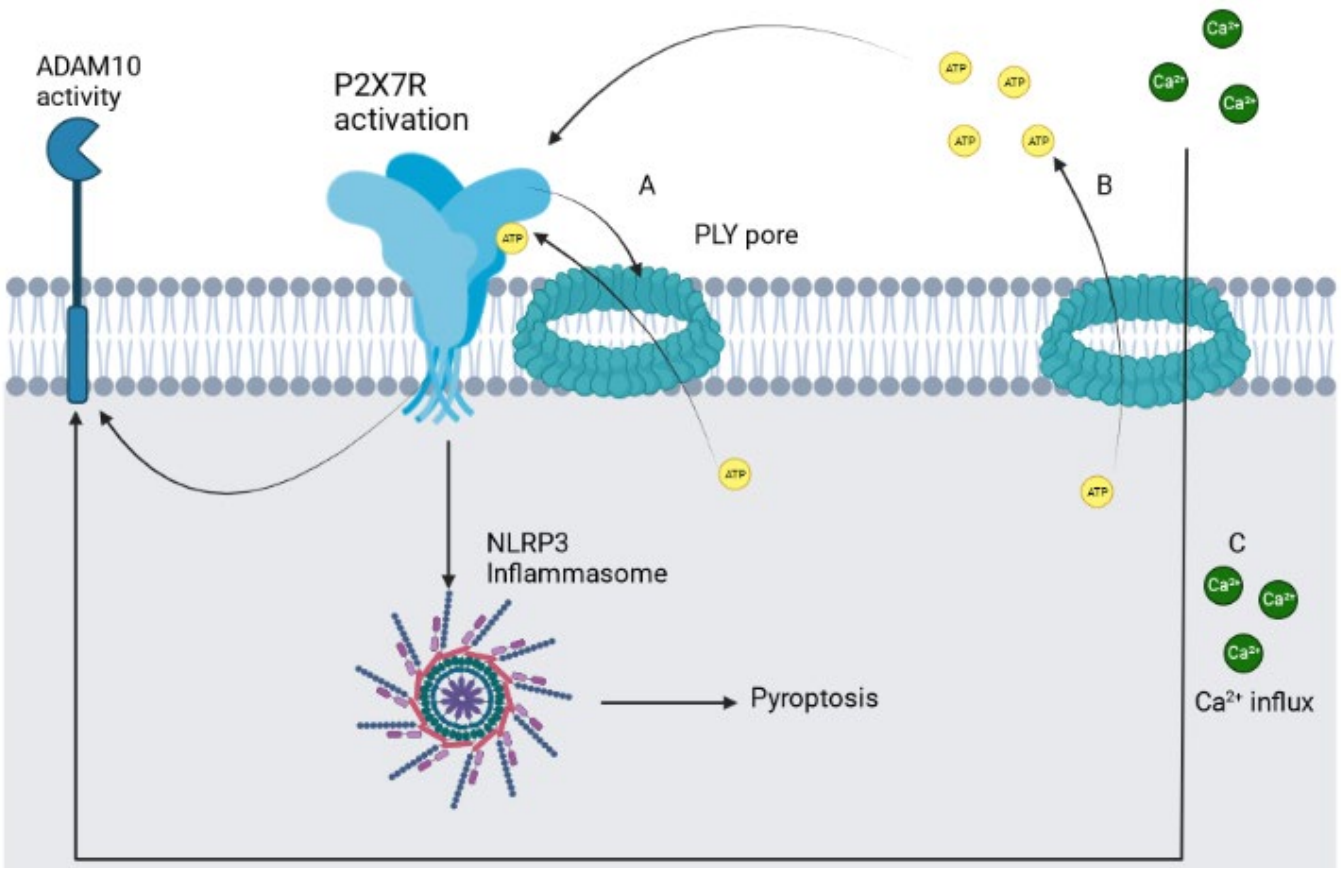

Figure 5 P2X7R might function as a proteinaceous receptor for PLY. *(A) In this hypothetical model P2X7R might function as a receptor for PLY, catalyzing its binding to cholesterol and the subsequent pore formation. (B) Alternatively, P2X7 might be indirectly activated as a result of increased extracellular ATP, which is released through the independently generated PLY pores. (C) Lastly, independent of P2X7, the Ca^{2+} influx generated by the PLY pore could directly activate ADAM10, possibly aggravating PLY cytotoxicity. Created with BioRender.com.*

Materials and methods

Reagent, Resource or Machinery	Source	Identifier
Antibodies		
PE anti-human CD156c (ADAM10) antibody	BioLegend	Cat # 352702
Purified Mouse IgG1, k Isotype Ctrl Antibody	BioLegend	Cat # 400102
Cell culture		
A-549		CVCL_0023
HaCaT		CVCL_0038
HEK293T		CVCL_0063
THP-1		CVCL_0006
U-937		CVCL_0007
Dulbeco's Modified Eagle Medium with Glutamax supplement	Thermo Fisher	Cat # 31966021
Fetal calf serum	Sigma-Aldrich	Cat # F7524
HEPES	Thermo Fisher	Cat # 15630080
Trypan blue	Merck	Cat # T8154-20ml
Trypsin-EDTA (0.25%), phenol red	Thermo Fisher	Cat # 25200056
Commercial kits		
CellTiter-Glo luminescent cell viability assay	Promega	Cat # G7570
GeneJET PCR Purification kit	Thermo Fisher	Cat # K0702
Neon™ Transfection system 10 ul kit	Thermo Fisher	Cat # MPK1025
QIFIKIT	DAKO	Cat # K0078
Wizard Genomic DNA purification kit	Promega	Cat # A1125
Machinery		
BIO-RAD TC20Automated Cell Counter	Bio-Rad	Cat # 1450102
CLARIOstar	BMG Labtech	N/A
FACSVerse™	BD Biosciences	N/A
MTS 2/4 digital microtiter shaker	IKA	Cat # 0003208000
Neon™ Transfection system	Thermo Fisher	Model MPK5000
Miscellaneous		
Formaldehyde, 10%, methanol free, Ultra Pure	Polysciences inc.	Cat # 040181
Human erythrocytes	Isolated in this lab form healthy donors	N/A
Human Serum Albumin	Alburex 20, 200 g/l	N/A
Poly-L-lysine solution, 0.1% (w/v) in H_2O	Sigma-Aldrich	Cat # 25988630
RPMI medium 1640	Thermo Fisher	Cat # 52400025
Rabbit erythrocytes	Isolated by the department of veterinary sciences, Utrecht University	N/A
Solid white Flat bottom 96 wells plate	Corning	Cat # 3917
Triton x-100	Promega	Cat # H5141
Primers		
Forward primer: CCTCAACAATATAAAAGGGCAATCCA	Synthego	N/A
Reverse primer: AAACTTGTGTGTGCGGTTGG	Synthego	N/A

Sequencing primer: GGTTGGAATTACCCTCACAATAAGTTTTAATA	Synthego	N/A
Proteins		
2X Phusion Green HS II High Fidelity PCR Master Mix	Thermo Fisher	Cat # F566L
Recombinant PLY	Recombinant PLY was kindly provided by Victor Torres (NYU, New York, USA)	
Recombinant AT	Recombinant AT was produced in-house by Tristan van der Linden, described elsewhere (33)	
TrueCut™ Cas9 Protein v2	Thermo Fisher	Cat # A36498
Synthetic guide RNA		
Mixture of three sgRNAs targeting ADAM10:	Synthego	N/A
• UGAAGGAUUAUCUUACAAUG		
• UUUUUUUUAUAGGUCAGUAU		
• UAGAUUUCCAUGCCCAUGGA		
Non-targeting control	Synthego	N/A
Software		
• FlowJo™	BD Biosciences	N/A
• GraphPad Prism 9	Dotmatics	N/A
• ICE CRISPR Analysis Tool	Synthego	N/A

Cell Culture

A549, HaCaT, HEK293T, THP-1, and U937 cells were cultured in complete medium Dulbecco's Modified Eagle Medium (DMEM) with GlutaMAX supplement (Thermo Fisher), supplemented with 10% Fetal Calf Serum (FCS, Sigma-Aldrich) and 25mM HEPES (Thermo Fisher). Cells were incubated at cell culture conditions, at 37 °C, 5% CO_2. Harvesting adherent cells for passaging was initiated by detaching the cells using 0,25% Trypsin-EDTA phenol red (Thermo Fisher). Trypsin was subsequently neutralized with complete medium. Based on the cell count and desired confluency, a specific portion of the cell suspension (harvested adherent cells or non-adherent cells) was passaged into a new flask containing fresh medium, with a total end volume of 30 ml.

Cell Surface Protein Expression Flow Cytometry

Adherent cells were harvested with 0,25% Trypsin-EDTA phenol red and neutralized with complete medium. A small aliquot of the homogenous cell mixture was stained with trypan blue (Merck) and counted using the BIO-RAD TC20 Automated Cell Counter (Bio-Rad). The appropriate number of suspended cells was aliquoted, centrifuged at 558g for 4 min, and resuspended in FACS buffer (RPMI medium 1640 (Thermo Fisher), 0,05% HSA (Alburex 20)) to $2*10^6$ viable cells/ml. For each condition 45 ul of the cell suspension was added to a U-shaped 96-wells plate. Either primary anti-human ADAM10 antibodies (Biolegend) or an isotype control (Biolegend) diluted in FACS buffer was added to the appropriate wells, with a final concentration of 2 ug/ml. Further controls included cells that were only stained with the secondary antibody or remained unstained. The plate was incubated for 30 minutes in the dark at 4 °C, shaking at 300 RPM (IKA). Samples were washed 2x with FACS buffer. For the quantitative experiments, QIFIKIT (DAKO) beads were prepared according to the instructions of the manufacturer and added to the 96-wells plate in separate wells. Secondary antibody from the QIFIKIT was added to the appropriate wells, with an end concentration of 8 ug/ml. The plate was subsequently incubated for 30 minutes in the dark at 4 °C, shaking at 300 RPM, and the samples were

washed 2x with FACS buffer. Finally, the samples were resuspended in FACS buffer supplemented with 1% formaldehyde (Polysciences inc.). The samples were measured on the BD FACSVerse™ (BD Biosciences) and analyzed according to the instructions of the manufacturer using FlowJo™.

Cytotoxicity assay

To mitigate evaporation of the cell-containing medium during incubation, the outer 2 rows and columns of the 96-wells plates were filled with PBS. Additionally, dummy plates filled with PBS were prepared, and each sample containing plate was placed in-between them. Prior to the assay, the flat bottom 96-wells plates for the HEK293T cells were pre-coated to increase cell-adherence. A volume of 50 ul of 0,01% poly-L-lysine (Sigma-Aldrich), diluted in MilliQ water, was added to each well and incubated for 5-10 min at room temperature. The solution was then aspirated, and the wells were washed using PBS. Adherent cells were harvested as previously described. The suspended adherent cells were centrifuged at 558g for 4 minutes. The supernatant was aspirated, and the cells were washed with PBS. Adherent cells were then resuspended in 1 ml of complete medium. A small aliquot of cells was stained and counted as previously described, and the remaining cells were subsequently diluted to $2*10^5$ cells/ml. 100 ul of this cell suspension was added to each well of the flat bottom 96-wells plate. After four hours of incubation at 37°C, 5% CO_2, complete medium was aspirated from the adherent cells and replaced with starvation medium (1% FCS 25mM HEPES DMEM + GlutaMAX). The plate was incubated for an additional 20 hours. For the non-adherent cells, the cell suspension was counted and the appropriate volume of cells representing $8*10^5$ cells was taken and centrifuged at 558g for 4 min. The supernatant was aspirated, and the pellet was washed with PBS. The pellet was subsequently reconstituted with starvation medium to $2*10^5$ cells/ml. 100 ul of this cell suspension was added to each well of the U-shaped 96-wells plate. The plate was incubated for 24 hours.

For non-adherent cells, the plates were first centrifuged at 558g for 4 min. For all plates the medium was then aspirated and replaced with a 2x serial dilution of PLY in starvation medium. The highest tested concentration of PLY was 5 ug/ml and 2,5 ug/ml for adherent and non-adherent cells respectively. For AT a 3x serial dilution was prepared with the highest tested concentration of 10 ug/ml. As a negative control, cells were incubated solely in starvation medium. The intoxicated cells were further incubated for 24 hours. Cell viability was subsequently measured using CellTiter-Glo luminescent cell viability assay (Promega). The CellTiter-Glo reagent was prepared according to the instructions of the manufacturer. 40 ul of the supernatant of adherent and non-adherent cells (centrifuged at 558g for 4 min) was removed. Subsequently, 60 ul of the prepared CellTiter-Glo reagent was added to the cells. The contents were mixed and incubated in the dark for 10 minutes at room temperature. 100 ul of the lysed cell mixture was transferred to a solid white flat bottom 96 wells plate (Corning). Luminescence was measured using the CLARIOstar (BMG LABTECH, Emission wavelength: 555 nm, Emission bandwidth: 70 nm, Gain: 3600, Focal Height: 11,5 mm), and normalized to the negative control.

Hemolysis

0,5 ml of rabbit and human erythrocytes were resuspended in 10 ml of DPBSB (PBS, 0,5% HSA). Cells were washed twice at 805g for 10 min and the pellet was resuspended in 1 ml of DPBSB. A small sample was diluted 1:100 and erythrocytes were counted using the BIO-RAD TC20 Automated Cell Counter. The washed stock of erythrocytes was diluted to $1*10^8$ cells/ml. 100 ul of erythrocytes were added to each well of a U-shaped 96-wells plate. Subsequently, 50 ul of 2x serial dilution of PLY, with the highest end concentration of 24 ng/ml, was added to the plated erythrocytes. For the negative control, no toxins were added to the erythrocytes. To determine the maximum hemolysis, 50 ul of 0,2% Triton-x 100 (Promega) was used as a positive control. The plate was incubated for 1 hour at 37°C, 5% CO_2, shaking at 300 RPM. After incubation, the plate was centrifuged at 500xg for 5 min, and 100 ul of supernatant was moved to a flat bottom 96-wells plate. The OD at 415 nm was then measured using the CLARIOstar. Hemolysis was described as a portion of the positive control.

Generation of ADAM10 knockout cell lines

A 24-well plate with 500 ul complete medium in each well was prepared and placed in the incubator to pre-warm at 37°C, 5% CO_2. For every reaction $1,2*10^5$ A549 cells or $2*10^5$ THP-1 cells were required. Cells were harvested as previously described and kept in complete medium. The following steps were then performed in a RNase free environment. Working stocks of 25 pMol/ul synthetic guide RNA (sgRNA) were prepared by reconstituting either a mixture of three different sgRNAs targeting ADAM10 (Synthego) or NTC sgRNA in 1x TE buffer. For each reaction, a TrueCut Cas9 protein + sgRNA solution was prepared, comprising 2000 ng of TrueCut Cas9 Protein v2 (Thermo Fisher) and 12 pMol TrueGuide gRNA (ADAM10 or NTC). The molar ratio of Cas9 protein and sgRNA was 1:1, and the combined volume of both components was less than 1/10th of the total reaction volume. This mixture was filled to a total volume of 5 ul using resuspension buffer R (Thermo Fisher). The Cas9 + sgRNA mixture was incubated at room temperature for 5-20 minutes. Cell preparation was finished by washing the cells with PBS (without Ca^{2+} and Mg^{2+}) at 400xg for 5 minutes and resuspending them in 5 ul resuspension buffer R for each reaction. Avoid storing the cell suspension for more than 15-30 minutes. The cell suspension was subsequently added to the formed ribonucleoprotein complexes. Cell transfection was carried out using the Neon™ Transfection system (Thermo Fisher) following the manufacturer's instructions. The following settings were used for A549 and THP-1 cells respectively: 1200 pulse voltage, 30 pulse width, 2 pulses; 1700 pulse voltage, 20 pulse width, 1 pulse. After transfection, the cells were moved to the pre-warmed 24-wells plate and incubated at 37%°C, 5% CO2.

Genetic DNA isolation, sequencing, and ICE analysis

$3*10^6$ cells were harvested as previously described and resuspended in 1ml complete medium. Genomic DNA isolation from tissue culture cells was performed using the Wizard Genomic DNA purification kit (Promega) according to the instructions of the manufacturer. Primers were reconstituted in MilliQ water to reach a stock concentration of 0,5 uM. 2X Phusion Green HS II High Fidelity PCR Master Mix (Thermo Fisher) was used to prepare the PCR mixture following the instructions of the manufacturer. The parameters on the T100™ Thermal Cycler (Bio-Rad) differing from the standard protocol were as follows: annealing temperature was set at 64,7°C for a duration of 30 seconds, extension time was established at 15 seconds, and a total of 35 cycles were performed. Gel electrophoresis confirmed the success of the PCR. The PCR product was purified using the GeneJET PCR Purification Kit (Thermo Fisher) according to the instructions of the manufacturer and send for sanger sequencing by Macrogen Europe. Analysis of the sequence was performed using the ICE CRISPR Analysis Tool of Synthego.

Supplementary

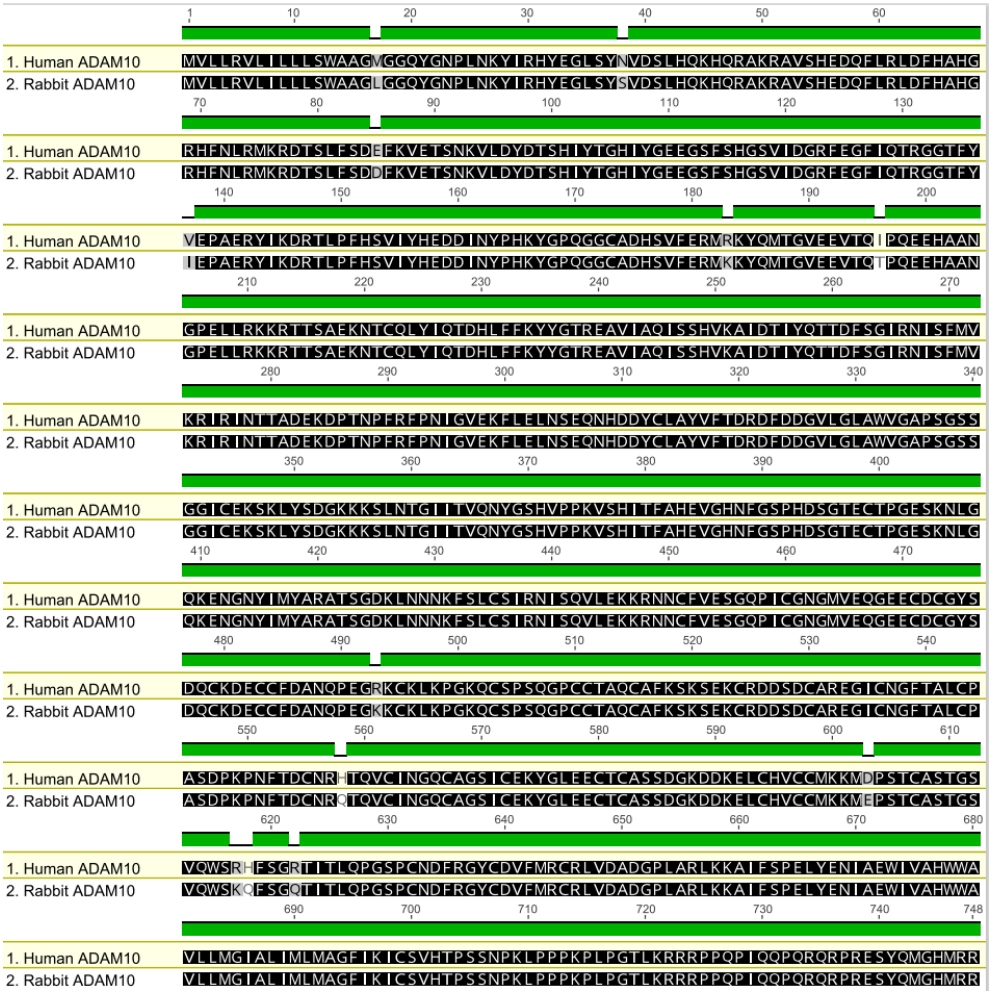

Figure S1 Rabbit ADAM10 aligned to human ADAM10. *The total length of the proteins is 748 amino acids. There are 736 (98.4%) identical sites between the two ADAM10 proteins. NCBI reference sequence: Human ADAM10 = NP_001101.1; Rabbit ADAM10 = XP_051677914.1. Geneious version 9.1 created by Biomatters. Available from http://www.geneious.com*

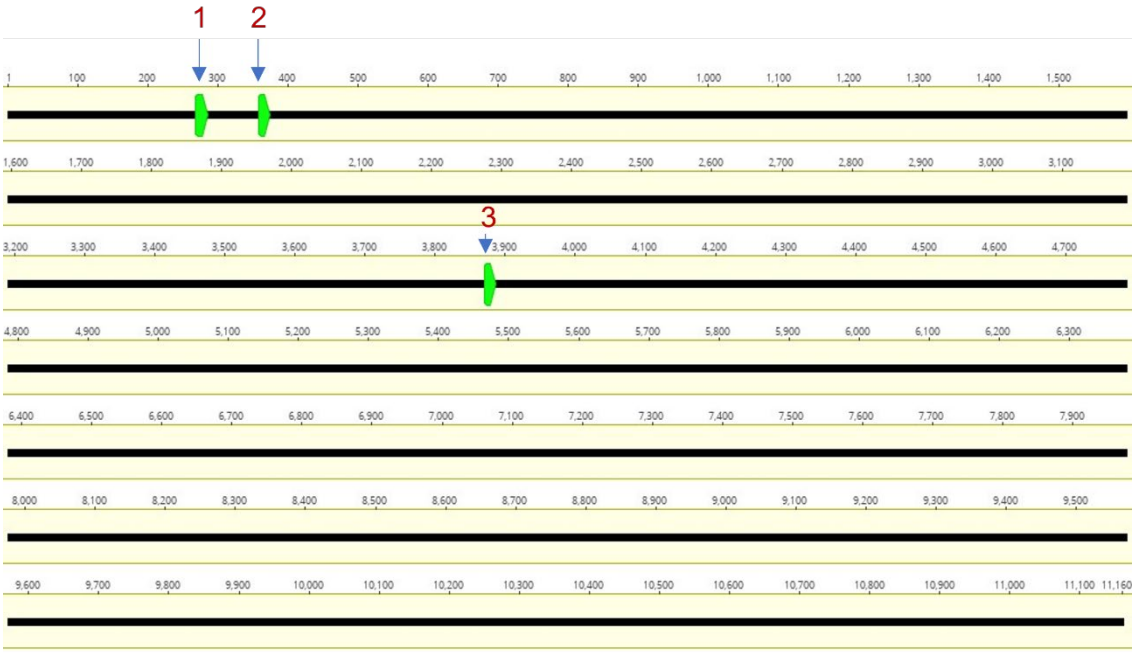

Figure S2 sgRNA aligned with ADAM10 mRNA. *Homo sapiens ADAM metallopeptidase domain 10 (ADAM10), transcript variant 1, mRNA (NCBI Reference Sequence: NM_001110.4) aligned with sgRNA 1 (UGAAGGAUUAUCUUACAAUG), sgRNA 2 (UUUUUUUUAUAGGUCAGUAU), and sgRNA 3 (UAGAUUUCCAUGCCCAUGGA). Geneious version 9.1 created by Biomatters. Available from http://www.geneious.com*

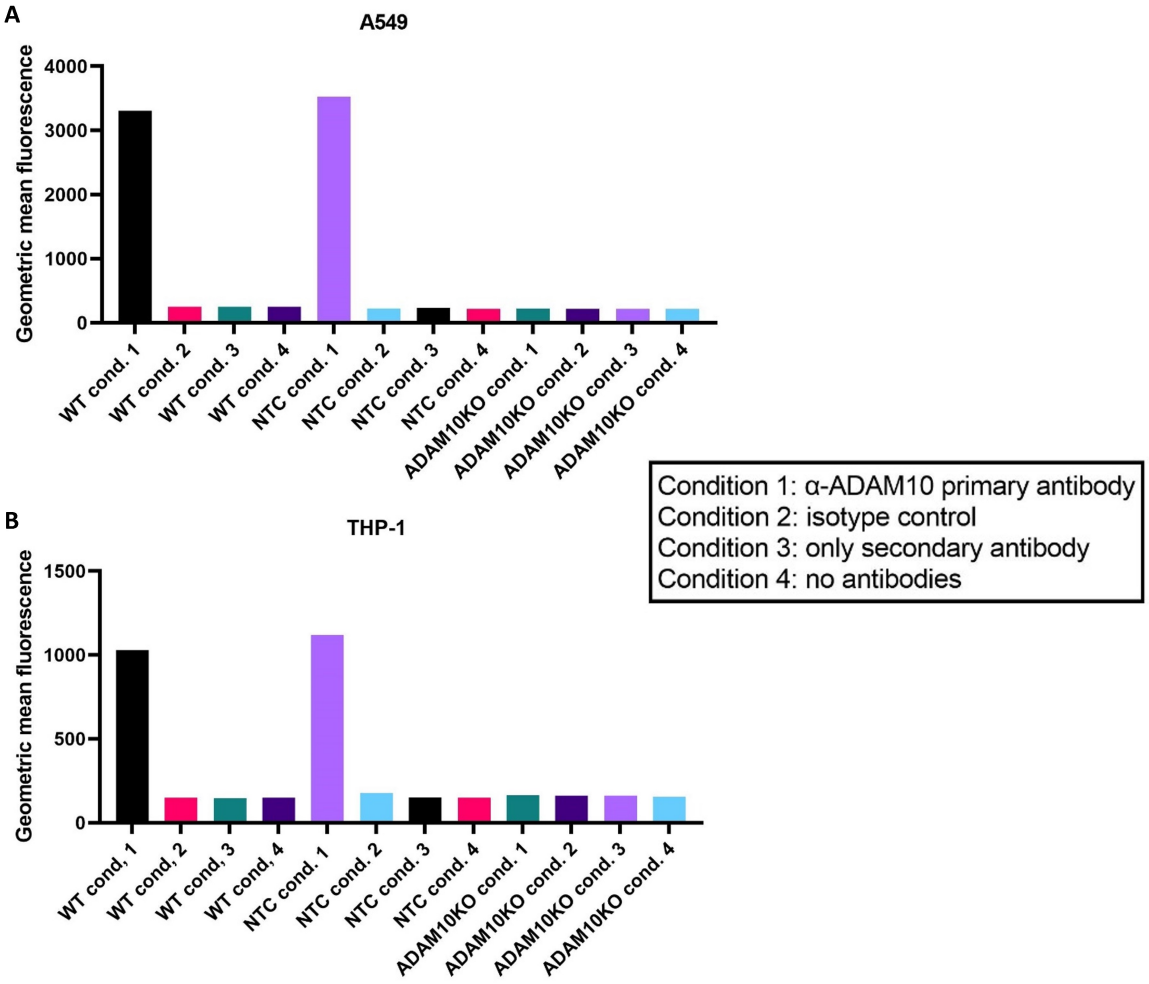

Figure S3 Geometric mean fluorescence of the WT, NTC and ADAM10KO Polyclonal populations. *Polyclonal NTC and ADAM10KO populations were validated using flow cytometry. Both populations depicted a similar geometric mean fluorescence (GMF) upon ADAM10 staining (condition 1) for the NTC and the WT cells. A clear decrease in GMF is observed in the ADAM10KO cells (condition 1) relative to the NTC and WT populations. This indicates that the knockout of ADAM10 was successful in most cells. Both the A549 (A) and THP-1 (B) populations demonstrated no aspecific antibody binding, as the GMF of the control conditions 2 and 3 is comparable to that of the unstained control (condition 4).*

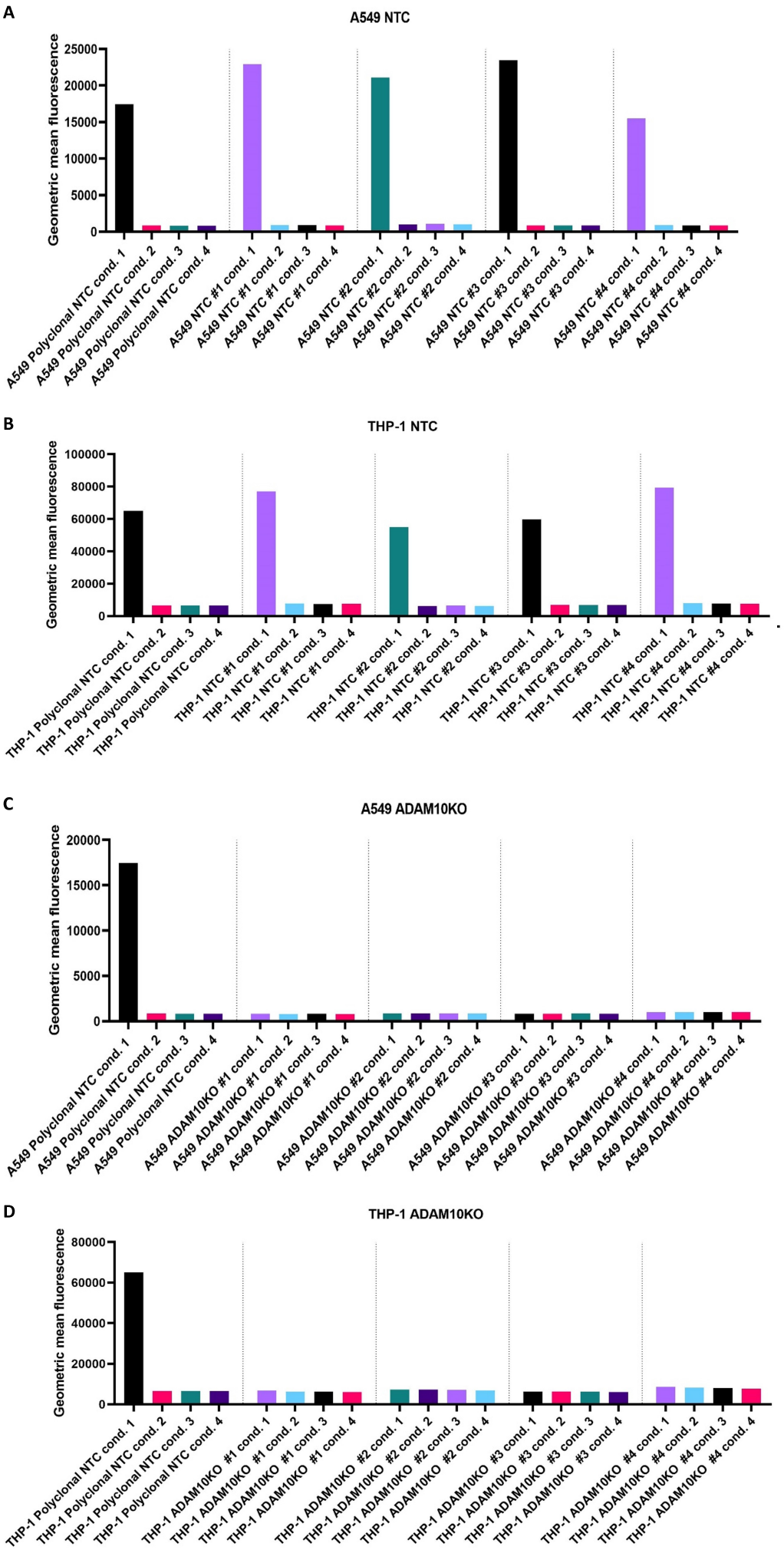

Condition 1: α-ADAM10 primary antibody
Condition 2: isotype control
Condition 3: only secondary antibody
Condition 4: no antibodies

Figure S4 Geometric mean fluorescence of NTC and ADAM10KO monoclonals. *Monoclonal NTC and ADAM10KO populations were validated using flow cytometry. Both cell lines exhibited similar phenotypical patterns. (A, B) With slight variance, the NTC populations showed comparable GMF to their respective polyclonal NTC population upon ADAM10 staining (condition 1). (C, D) A clear decrease in GMF is observed in the ADAM10KO cells (condition 1) relative to the polyclonal NTC population. This indicates that the knockout of ADAM10 was successful in the selected cells. The populations demonstrated no aspecific antibody binding, as the GMF of the control conditions 2 and 3 is comparable to the unstained control (condition 4).*

A

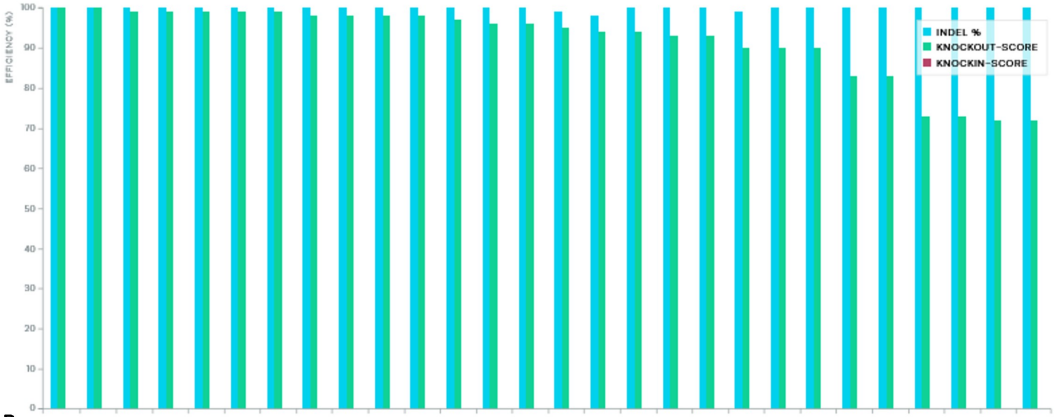
EFFICIENCY (%)
INDEL %
KNOCKOUT-SCORE
KNOCKIN-SCORE

B

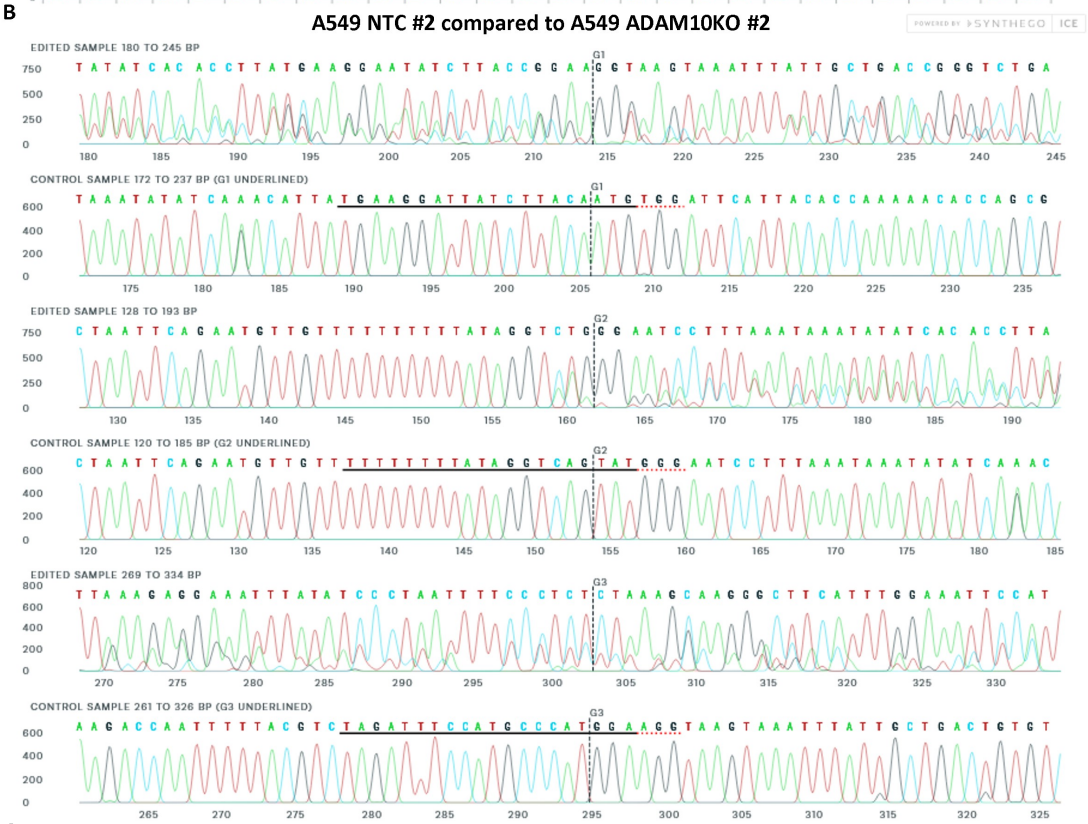
A549 NTC #2 compared to A549 ADAM10KO #2
EDITED SAMPLE 180 TO 245 BP
CONTROL SAMPLE 172 TO 237 BP (G1 UNDERLINED)
EDITED SAMPLE 128 TO 193 BP
CONTROL SAMPLE 120 TO 185 BP (G2 UNDERLINED)
EDITED SAMPLE 269 TO 334 BP
CONTROL SAMPLE 261 TO 326 BP (G3 UNDERLINED)

C

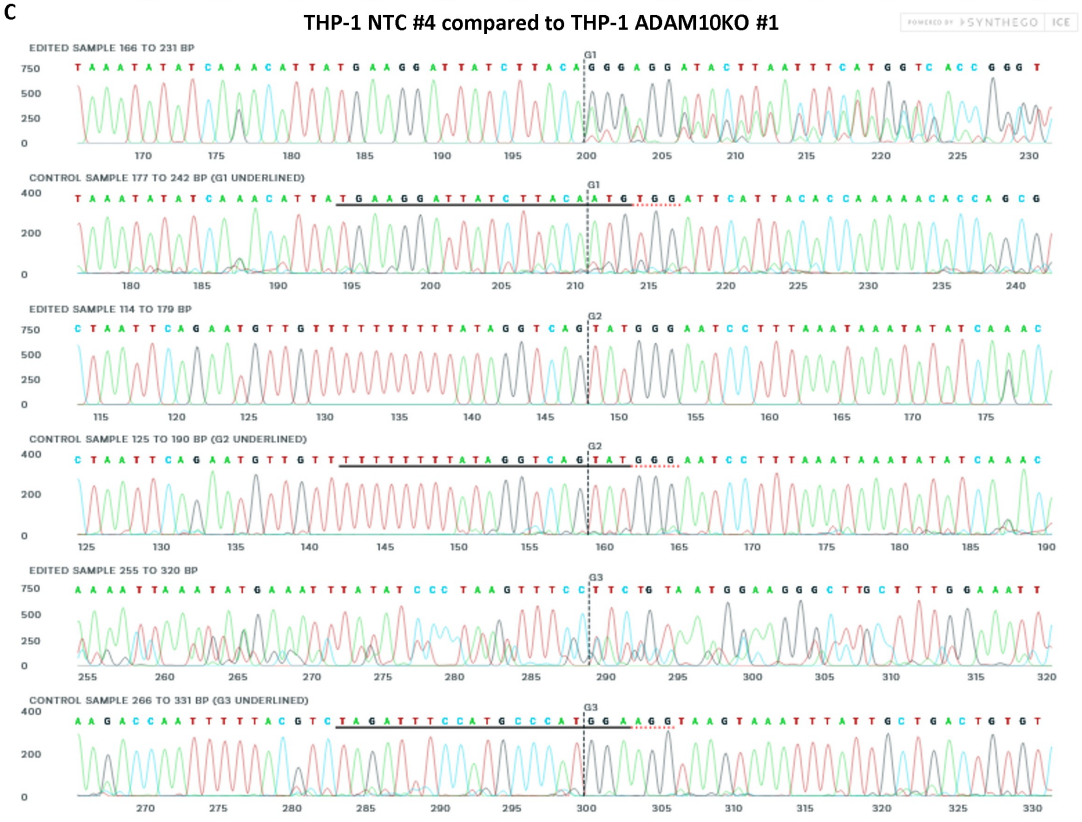
THP-1 NTC #4 compared to THP-1 ADAM10KO #1
EDITED SAMPLE 166 TO 231 BP
CONTROL SAMPLE 177 TO 242 BP (G1 UNDERLINED)
EDITED SAMPLE 114 TO 179 BP
CONTROL SAMPLE 125 TO 190 BP (G2 UNDERLINED)
EDITED SAMPLE 255 TO 320 BP
CONTROL SAMPLE 266 TO 331 BP (G3 UNDERLINED)

Figure S5 ICE analysis of A549 and THP-1 monoclonal ADAM10 PCR product. *(A) The general overview of compared samples reveals a 100% indel% for every comparison. The knockout score differs between samples (deletion of more than 21 base pairs). NTC and ADAM10KO pairings were selected on a high knockout score. (B) Traces of A549 NTC #2 as control sample compared to traces of A549 ADAM10KO #2 as edited sample. Clear editing occurred at the sites of sgRNA homology. (C) Traces of THP-1 NTC #4 as control sample compared to traces of THP-1 ADAM10KO #1 as edited sample. Clear editing occurred at the sites of sgRNA homology.*

A

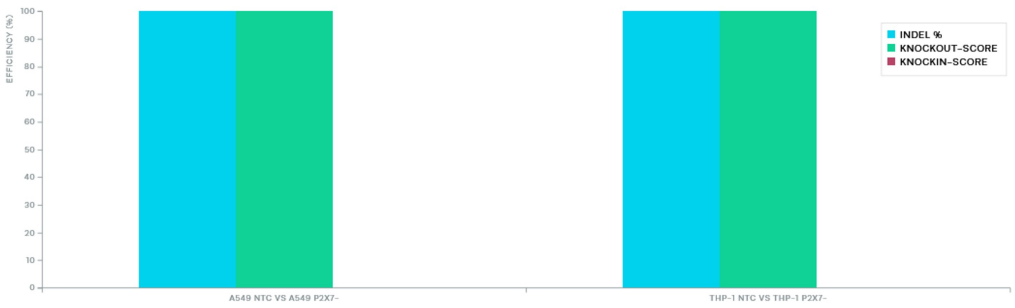

B

A549 NTC compared to A549 P2X7KO

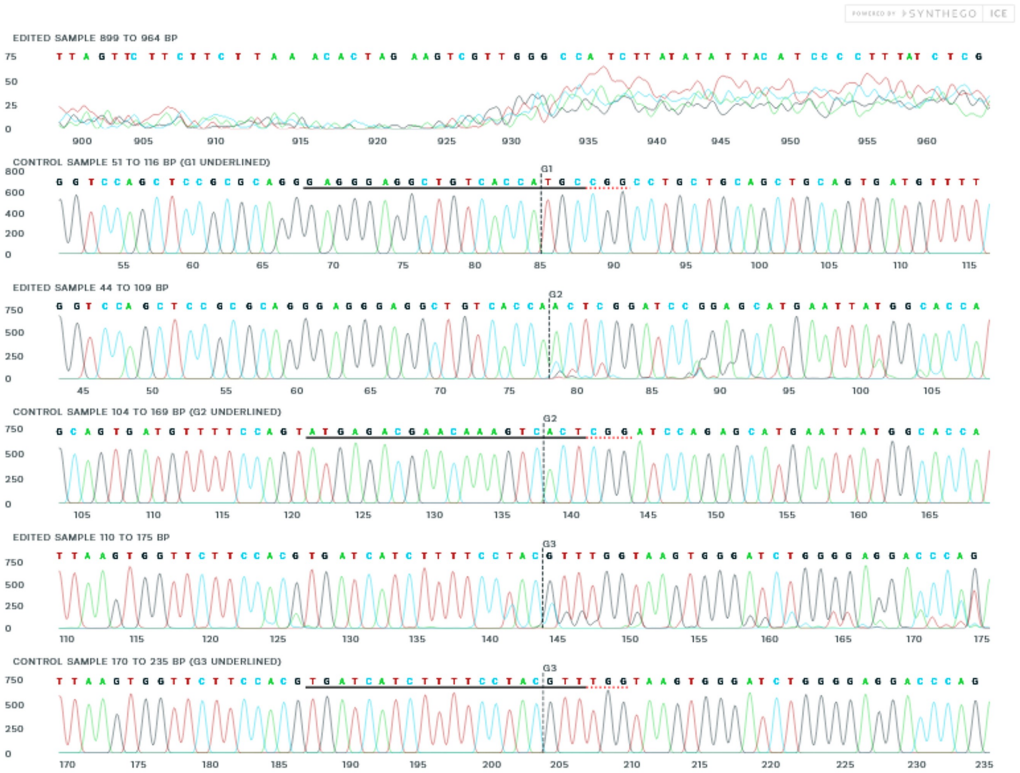

C

THP-1 NTC compared to THP-1 P2X7KO

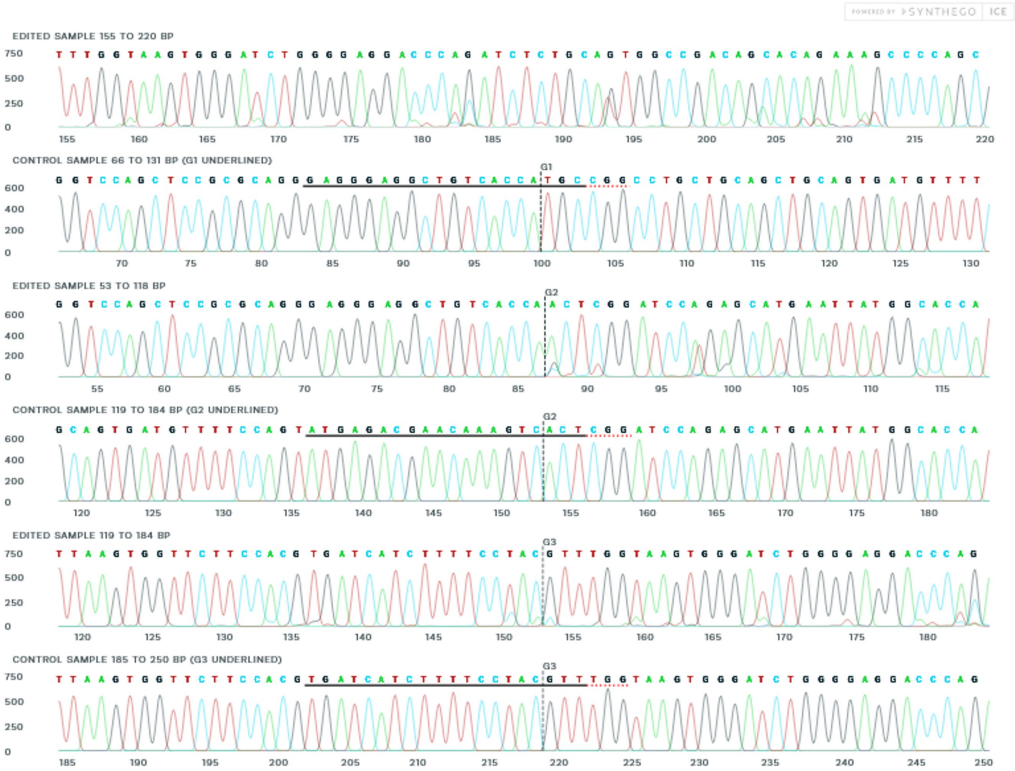

Figure S6 ICE analysis of A549 and THP-1 polyclonal P2X7 PCR product. *(A) The general overview of compared samples reveals a 100% indel% and knockout score for both the THP-1 and A549 NTC vs P2X7KO comparisons. (B) Traces of A549 NTC as control sample compared to traces of A549 P2X7KO as edited sample. Editing occurred at the sites of sgRNA homology. (C) Traces of THP-1 NTC as control sample compared to traces of THP-1 P2X7KO as edited sample. Limited editing occurred at the sites of sgRNA homology.*

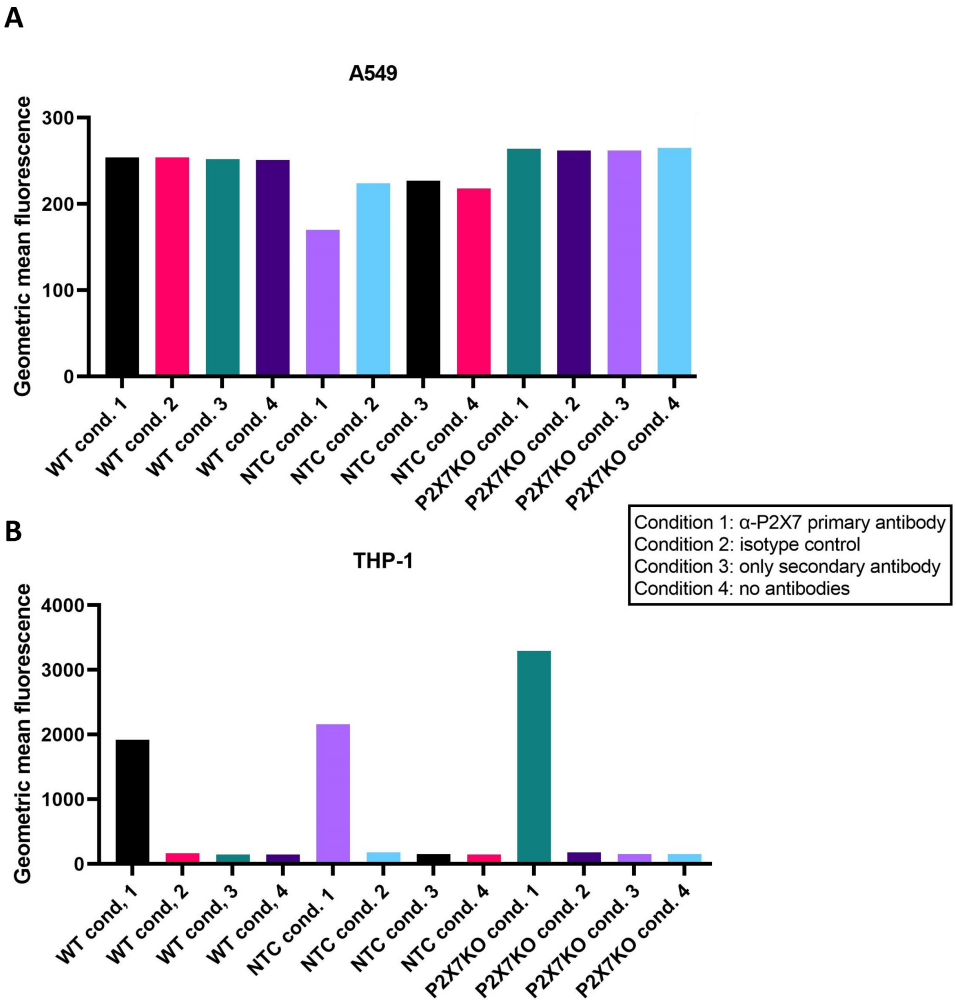

Figure S7 Geometric mean fluorescence of the WT, NTC and P2X7KO Polyclonal populations. *Polyclonal NTC and P2X7KO populations were validated using flow cytometry. Both populations depicted a similar geometric mean fluorescence(GMF) upon ADAM10 staining (condition 1) for the NTC and the WT. No decrease in GMF is observed in the P2X7KO cells (condition 1) relative to the NTC and WT populations. This indicates that the knockout of P2X7 was unsuccessful in most cells. Both the A549 (A) and THP-1 (B) populations demonstrated no aspecific antibody binding, as the GMF of the control conditions 2 and 3 is comparable to that of the unstained control (condition 4).*

Bibliography

1. Weiser JN, Ferreira DM, Paton JC. Streptococcus pneumoniae: Transmission, colonization and invasion [Internet]. Vol. 16, Nature Reviews Microbiology. Nature Publishing Group; 2018 [cited 2022 Aug 14]. p. 355–67. Available from: www.nature.com/nrmicro
2. Maestro B, Sanz JM. Choline binding proteins from Streptococcus pneumoniae: A dual role as enzybiotics and targets for the design of new antimicrobials [Internet]. Vol. 5, Antibiotics. MDPI AG; 2016 [cited 2023 Jul 6]. Available from: /pmc/articles/PMC4929436/
3. Rubins JB, Janoff EN. Pneumolysin: A multifunctional pneumococcal virulence factor. J Lab Clin Med. 1998;131(1):21–7.
4. Pereira JM, Xu S, Leong JM, Sousa S. The Yin and Yang of Pneumolysin During Pneumococcal Infection. Front Immunol. 2022;13(April):1–21.
5. Peraro MD, Van Der Goot FG. Pore-forming toxins: Ancient, but never really out of fashion. Nat Rev Microbiol. 2016;14(2):77–92.
6. Van Pee K, Mulvihill E, Müller DJ, Yildiz Ö. Unraveling the Pore-Forming Steps of Pneumolysin from Streptococcus pneumoniae. Nano Lett [Internet]. 2016 Dec 14 [cited 2023 Jul 10];16(12):7915–24. Available from: https://pubs.acs.org/sharingguidelines
7. Gilbert RJC, Sonnen AFP. Measuring kinetic drivers of pneumolysin pore structure. Eur Biophys J [Internet]. 2016 May 1 [cited 2023 Jul 10];45(4):365–76. Available from: https://link-springer-com.proxy.library.uu.nl/article/10.1007/s00249-015-1106-x
8. Rojko N, Anderluh G. How Lipid Membranes Affect Pore Forming Toxin Activity. Acc Chem Res [Internet]. 2015 Dec 7 [cited 2023 Jul 10];48(12):3073–9. Available from: https://pubs.acs.org/sharingguidelines
9. Möckl L. The Emerging Role of the Mammalian Glycocalyx in Functional Membrane Organization and Immune System Regulation. Vol. 8, Frontiers in Cell and Developmental Biology. Frontiers Media S.A.; 2020. p. 529506.
10. Inoshima I, Inoshima N, Wilke GA, Powers ME, Frank KM, Wang Y, et al. A Staphylococcus aureus pore-forming toxin subverts the activity of ADAM10 to cause lethal infection in mice. Nat Med. 2011;17(10):1310–4.
11. Liao S, Lin Y, Liu L, Yang S, Lin YY, He J, et al. ADAM10-a “multitasker” in sepsis: focus on its posttranslational target [Internet]. Vol. 72, Inflammation Research. Springer Science and Business Media Deutschland GmbH; 2022 [cited 2023 Jul 6]. p. 395. Available from: /pmc/articles/PMC9789377/
12. Lieber M, Todaro G, Smith B, Szakal A, Nelson-Rees W. A continuous tumor-cell line from a human lung carcinoma with properties of type II alveolar epithelial cells. Int J Cancer [Internet]. 1976 Jan 15 [cited 2023 Aug 10];17(1):62–70. Available from: https://onlinelibrary.wiley.com/doi/10.1002/ijc.2910170110
13. Boukamp P, Petrussevska RT, Breitkreutz D, Hornung J, Markham A, Fusenig NE. Normal keratinization in a spontaneously immortalized aneuploid human keratinocyte cell line. J Cell Biol [Internet]. 1988 Mar 1 [cited 2023 Aug 10];106(3):761–71. Available from: http://rupress.org/jcb/article-pdf/106/3/761/1461052/761.pdf
14. Ndiaye C, Bassene H, Lagier JC, Raoult D, Sokhna C. Asymptomatic carriage of Streptococcus pneumoniae detected by qPCR on the palm of hands of populations in rural Senegal. PLoS Negl Trop Dis [Internet]. 2018 Dec 1 [cited 2023 Jul 13];12(12). Available from: /pmc/articles/PMC6312329/
15. Lin YC, Boone M, Meuris L, Lemmens I, Van Roy N, Soete A, et al. Genome dynamics of the human embryonic kidney 293 lineage in response to cell biology manipulations. Nat Commun [Internet]. 2014 Sep 3 [cited 2023 Aug 10];5(1):12. Available from: www.nature.com/naturecommunications
16. Sundström C, Nilsson K. Establishment and characterization of a human histiocytic lymphoma cell line (U-937). Int J Cancer [Internet]. 1976 May 15 [cited 2023 Aug 10];17(5):565–77. Available from: https://onlinelibrary.wiley.com/doi/10.1002/ijc.2910170504
17. Tsuchiya S, Yamabe M, Yamaguchi Y, Kobayashi Y, Konno T, Tada K. Establishment and characterization of a human acute monocytic leukemia cell line (THP-1). Int J Cancer [Internet]. 1980 Aug 15 [cited 2023 Aug 10];26(2):171–6. Available from: https://onlinelibrary.wiley.com/doi/10.1002/ijc.2910260208
18. Larpin Y, Besançon H, Iacovache MI, Babiychuk VS, Babiychuk EB, Zuber B, et al. Bacterial pore-forming toxin pneumolysin: Cell membrane structure and microvesicle shedding capacity determines differential survival of immune cell types. FASEB J. 2020;34(1):1665–78.
19. Dreymueller D, Uhlig S, Ludwig A. ADAM-family metalloproteinases in lung inflammation: potential therapeutic targets. Am J Physiol Cell Mol Physiol [Internet]. 2015 Feb 15 [cited 2023 Jul 26];308(4):L325–43. Available from: https://www.physiology.org/doi/10.1152/ajplung.00294.2014

20. Taddei M, Giannoni E, Fiaschi T, Chiarugi P. Anoikis: an emerging hallmark in health and diseases. J Pathol [Internet]. 2012 Jan 1 [cited 2023 Jul 31];226(2):380–93. Available from: https://onlinelibrary.wiley.com/doi/10.1002/path.3000
21. Yilmaz M, Christofori G. EMT, the cytoskeleton, and cancer cell invasion [Internet]. Vol. 28, Cancer and Metastasis Reviews. Springer; 2009 [cited 2023 Jul 31]. p. 15–33. Available from: https://link-springer-com.proxy.library.uu.nl/article/10.1007/s10555-008-9169-0
22. Desouza M, Gunning PW, Stehn JR. The actin cytoskeleton as a sensor and mediator of apoptosis. Bioarchitecture [Internet]. 2012 May 5 [cited 2023 Jul 31];2(3):75–87. Available from: /pmc/articles/PMC3414384/
23. Yuksel H, Ocalan M, Yilmaz O. E-Cadherin: An Important Functional Molecule at Respiratory Barrier Between Defence and Dysfunction [Internet]. Vol. 12, Frontiers in Physiology. Frontiers Media S.A.; 2021 [cited 2023 Jul 26]. Available from: /pmc/articles/PMC8521047/
24. Yuan Q, Yu H, Chen J, Song X, Sun L. ADAM10 promotes cell growth, migration, and invasion in osteosarcoma via regulating E-cadherin/β-catenin signaling pathway and is regulated by miR-122-5p. Cancer Cell Int [Internet]. 2020 Mar 30 [cited 2023 Jul 26];20(1):99. Available from: https://cancerci.biomedcentral.com/articles/10.1186/s12935-020-01174-2
25. Hoven G Von, Qin Q, Neukirch C, Husmann M, Hellmann N. S. aureus α-toxin: Small pore, large consequences [Internet]. Vol. 400, Biological Chemistry. De Gruyter; 2019 [cited 2023 Aug 2]. p. 1261–76. Available from: https://www-degruyter-com.proxy.library.uu.nl/document/doi/10.1515/hsz-2018-0472/html
26. Di Virgilio F, Dal Ben D, Sarti AC, Giuliani AL, Falzoni S. The P2X7 Receptor in Infection and Inflammation. Vol. 47, Immunity. Cell Press; 2017. p. 15–31.
27. Zhang W jun, Luo C, Huang C, Pu F qin, Zhu J feng, Zhu Z ming. PI3K/Akt/GSK-3β signal pathway is involved in P2X7 receptor-induced proliferation and EMT of colorectal cancer cells. Eur J Pharmacol. 2021 May 15;899:174041.
28. Pupovac A, Foster CM, Sluyter R. Human P2X7 receptor activation induces the rapid shedding of CXCL16. Biochem Biophys Res Commun. 2013 Mar 22;432(4):626–31.
29. Domon H, Oda M, Maekawa T, Nagai K, Takeda W, Terao Y. Streptococcus pneumoniae disrupts pulmonary immune defence via elastase release following pneumolysin-dependent neutrophil lysis. Sci Rep. 2016;6(November):1–13.
30. ADAM10 - Disintegrin and metalloproteinase domain-containing protein 10 - Homo sapiens (Human) | UniProtKB | UniProt [Internet]. [cited 2023 Aug 2]. Available from: https://www.uniprot.org/uniprotkb/O14672/entry
31. Zafar MA, Wang Y, Hamaguchi S, Weiser JN. Host-to-Host Transmission of Streptococcus pneumoniae Is Driven by Its Inflammatory Toxin, Pneumolysin. Cell Host Microbe [Internet]. 2017;21(1):73–83. Available from: http://dx.doi.org/10.1016/j.chom.2016.12.005
32. Wilke GA, Wardenburg JB. Role of a disintegrin and metalloprotease 10 in Staphylococcus aureus α-hemolysin - Mediated cellular injury. Proc Natl Acad Sci U S A [Internet]. 2010 Jul 27 [cited 2023 Aug 2];107(30):13473–8. Available from: https://www-pnas-org.proxy.library.uu.nl/doi/abs/10.1073/pnas.1001815107
33. Winter SV, Zychlinsky A, Bardoel BW. Genome-wide CRISPR screen reveals novel host factors required for Staphylococcus aureus α-hemolysin-mediated toxicity. Sci Rep [Internet]. 2016;6(December 2015):1–9. Available from: http://dx.doi.org/10.1038/srep24242